STMN2 mediates nuclear translocation of Smad2/3 and enhances TGFβ signaling by destabilizing microtubules to promote epithelial-mesenchymal transition in hepatocellular carcinoma

Fang-Jing Zhong, Bo Sun, Mo-Mo Cao, Cong Xu, Yi-Ming Li, Lian-Yue Yang [*]

Liver Cancer Laboratory, Department of Surgery, Xiangya Hospital, Central South University, Changsha, 410008, Hunan, China

A B S T R A C T

Metastasis remains the major obstacle of improving the survival of patients with hepatocellular carcinoma (HCC). Epithelial–mesenchymal transition (EMT) is critical to cancer metastasis. Successful induction of EMT requires dramatic cytoskeleton rearrangement. However, the significance of microtubule (MT), one of the core components of cell cytoskeleton, in this process remains largely unknown. Here we revealed that STMN2, an important MT dynamics regulator, is barely expressed in normal live tissues but markedly up-regulated in HCCs, especially in those with early recurrence. High STMN2 expression correlates with aggressive clinicopathological features and predicts poor prognosis of HCC patients. STMN2 overexpression in HCC cells promotes EMT, invasion and metastasis *in vitro* and *in vivo*, whereas STMN2 knockdown has opposite results. Mechanistically, STMN2 modulates MTs disassembly, disrupts MT-Smad complex, and facilitates release from MT network, phosphorylation and nuclear translocation of Smad2/3 even independent of TGFβ stimulation, thereby enhancing TGFβ signaling. Collectively, STMN2 orchestrates MT disassembly to facilitate EMT via TGF-β signaling, providing a novel insight into the mechanisms underlying cancer metastasis. STMN2 is a promising prognostic biomarker and potential therapeutic target for HCC.

1. Introduction

Hepatocellular carcinoma (HCC) is the sixth most common cancer and the fourth leading cause of cancer-related death globally [1]. Despite the substantial progress in surveillance and treatment, the long survival of HCC still remains dismal, mainly due to the frequent metastasis and recurrence [2]. However, to date, effective strategies to prevent cancer metastasis are still lacking. Therefore, comprehensive elucidation of the molecular mechanisms underlying HCC metastasis is urgently needed.

Epithelial-mesenchymal transition (EMT) has been wildly demonstrated to be crucial for the invasion-metastasis cascade in various cancers including HCC [3,4]. During EMT, epithelial cells undergo dramatic cytoskeleton rearrangement and transform into mesenchymal phenotype with a spindle-like cell shape and increased migratory and invasive capabilities [5]. Cell cytoskeleton consists of actin filament (F-actin), microtubule (MT) and intermediate filament [6]. However, most present studies have mainly focused on the contributions of F-actin

dynamics to EMT [5,7,8], and the significance of MT in this process still remains largely unknown.

MT is a highly dynamic polymer of αβ-tubulin heterodimers, with the plus end undergoing dramatic switch between tubulin assembly and disassembly, a behavior named dynamic instability [9]. MT rearrangement depends greatly on this behavior and is critically involved in various cellular processes, including cell shape, cell motility and intracellular signal transduction [6,9,10]. It is noteworthy that the dynamic instability is closely regulated by the stathmin family proteins [9,11,12].

Stathmin family proteins, serving as major MT destabilizing factors, play a critical role in MT disassembly and dynamics [11,12]. This family consists of four members, namely STMN1-4 [11]. Among these, STMN2 (also named SCG10) is of particular interest. In contrast to the other three members, STMN2 is highly expressed in embryos, but dramatically reduced in adults [13,14]. Moreover, the mRNA level of STMN2 is significantly up-regulated in HCC tissues according to the Oncomine database. Functionally, STMN2, as a MT destabilizer, is critically involved in neurite extension and cell motility [12,13,15,16]. Noticeably, ectopic expression of STMN2 in adult liver induces organ fibrosis

---

List of abbreviations

STMN2	stathmin 2
HCC	hepatocellular carcinoma
EMT	epithelial-mesenchymal transition
MT	microtubule
ANLT	adjacent nontumor liver tissue
NLT	normal liver tissue
OS	overall survival
DFS	disease free survival
TGFβ	transforming growth factor beta
Smad2/3	smad family member 2/3
TβRI	transforming growth factor beta receptor type I
TTK	TTK protein kinase
TCGA	The Cancer Genome Atlas

by facilitating the hepatic stellate cell phenotype change from quiescent fat-storing cell to mobile myofibroblast-like cell [15], a similar phenomenon of EMT process [17]. Additionally, a few emerging evidences indicate that MT destabilization is required for EMT process [18–20]. These findings have greatly aroused our interest in the role of STMN2 in HCC progression, especially EMT.

In this study, we revealed that STMN2 is frequently up-regulated in HCC and predicts poor prognosis of HCC patients. Furthermore, STMN2 promotes HCC cell EMT, invasion and metastasis *in vitro* and *in vivo*. Mechanistically, through modulating MTs disassembly, STMN2 disrupts the complex between Smads and MTs, and facilitates the dissociation of Smad2/3 from MT network and phosphorylation and nuclear translocation of these proteins even independent of TGFβ stimulation, thereby facilitating TGFβ signaling and consequent EMT and metastasis.

2. Materials and methods

2.1. Patients and tissue specimens

This study was approved by both of the Ethics Committee of Xiangya Hospital, Central South University (CSU) and the Affiliated Cancer Hospital of Xiangya School of Medicine, CSU. Informed consent was obtained from each patient before study. 30 pairs of frozen fresh HCC specimens and adjacent nontumor liver tissues (ANLTs) for quantitative real-time PCR (qRT-PCR) and western blot analyses were obtained between January 2011 and December 2013 at the Department of Surgery, Xiangya Hospital. 136 pairs of paraffin-embedded HCCs and ANLTs in training cohort and 54 paraffin-embedded normal liver tissues were collected from HCC and hepatic hemangioma patients respectively, who had undergone curative resection at the Department of Surgery, Xiangya Hospital from February 2006 to December 2010. In addition, 102 pairs of paraffin-embedded HCCs and ANLTs in validation cohort and 35 paraffin-embedded normal liver tissues were correspondingly obtained from HCC and hepatic hemangioma patients, who had received curative resection at the Department of Abdominal Surgical Oncology, the Affiliated Cancer Hospital of Xiangya School of Medicine from January 2006 to December 2010. The diagnosis of patients was confirmed by two independent pathologists. The details for the patient enrollment are shown in Supplementary Fig. 1A. The clinicopathological features of these patients are listed in Supplementary Table 1. The follow-up procedures were regularly performed as our previous study described [21]. Research protocols was performed in strict compliance with the REMARK guidelines for reporting prognostic biomarkers in cancer [22].

2.2. Cell lines and cell culture

The source of cell lines used in this study were described previously

[23]. Cells were maintained in Dulbecco's Modified Eagle's Medium (BioInd, Beit Haemek, Israel) supplemented with 10% fetal bovine serum (BioInd) and 1% penicillin-streptomycin (BioInd) at 37 °C with humidified atmosphere and 5% CO2.

2.3. RNA extraction and quantitative real-time PCR(qRT-PCR)

Total RNA was extracted from frozen tissues or cells using Trizol reagent (Life Technologies, Carlsbad, CA) according to the manufacturer's protocol. cDNA was synthesized using universal cDNA synthesis kit (Toyobo, tokyo, Japan) and subsequently subjected to quantitative real-time PCR (qRT-PCR) using SYBR Green PCR Kit (Roche Life Sciences, Switzerland). qRT-PCR was performed on PRISM 7300 Sequence Detection System (Applied Biosystems, CA) and done in triplicate. The relative fold change of target gene was normalized to GAPDH expression and calculated using $2^{-\Delta\Delta Ct}$ method. All the primer sequences are listed in Supplementary Table 4.

2.4. Western blot

Total protein was harvested using RIPA lysis buffer (CWBIO, Beijing, China), and cytoplasmic/nuclear protein were extracted by NE-PER™ Nuclear Cytoplasmic Extraction Reagent kit (Thermo Scientific, MA) according to the manufacturer's instructions. Identical quantities of proteins were separated by 10% sodium dodecyl sulfate-polyacrylamide gel electrophoresis (SDS-PAGE) and then transferred onto PVDF membrane (Millipore, Bedford, MA). After blocking with 5% skim milk, the membranes were incubated with primary antibodies overnight at 4 °C and then treated with HRP-conjugated secondary antibodies at room temperature for 30 min. The protein bands were visualized and imaged by ChemiDocTM Touch Imaging System (BIO-RAD, CA) using enhanced chemiluminescence regents (Thermo Scientific, MA). The antibodies are presented in Supplementary Tables 5 and 6

2.5. Immunohistochemistry (IHC)

IHC assay were performed with Universal two-step detection kit (ZSGB-BIO, Beijing, China) according to the procedure described previously [23]. Briefly, after antigen retrieval in microwave, the sections were incubated with primary antibodies in a humidified chamber at 4 °C overnight. Then the sections were incubated with HRP conjugated secondary antibody for 30 min at room temperature and subjected to DAB treatment, followed by counterstaining with hematoxylin, dehydrating in graded alcohols and mounting. Negative controls were included in all assays. The antibodies were listed in the Supplementary Table 4. IHC staining was scored basing on the staining intensity and percentage of positive cells. IHC staining score (IS) = SI (staining intensity) × PP (percentage of positive cells); SI was scored as 0 (negative) 1 (weak), 2 (moderate) and 3 (intense); PP was categorized as score 0 (<5%), 1 (5–25%), 2 (25–50%), 3 (50–75%) and 4 (>75%); IHC staining scoring 2 or less was defined as low expression and 3–12 as high expression [24].

2.6. Vector construction and transfection

The ectopic expression and knockdown lentivirus as well as control lentivirus were all purchased from Vigene Biosciences (Jinan, China). For overexpression studies, full length cDNA of STMN2 was inserted into lentiviral vectors. To knockdown STMN2 in HCC cells, three shRNA target sequences (shRNA1: 5′- GCTGAAACAATTGGCAGAGAA -3′, shRNA2: 5′- GGCTAATCTAGCTGCTATTAT -3′, shRNA3: 5′-GCTGATCTTGAAGCCACCATC-3′) were designed. The pLent-2in1shRNA-GFP-Puro lentiviral vector was applied to delete smad2/3, which contained both H1 promoter- and U6 promoter-driven cassettes and could simultaneously express shSmad2 (5′-GGATGAAGTATGTG-TAAAC-3′) and shSmad3 (5′-GGATTGAGCTGCACCTGAATG-3′) [25]. Lentivirus transfection was performed according to the manufacturer's

instructions. Stable clones were selected using 2 μg/ml puromycin (Sigma-Aldrich, St. Louis, MO). The siRNA targeting TTK (5′-GUGGCAGAGAAUUGACAAUTT-3′) was purchased from Gene-Pharma (Shanghai, China) and transfection was conducted with Lipofectamine 2000 (Invitrogen) following the manufacturer's instruction. Overexpression or depletion of target genes was verified by qRT-PCR and/or Western blot.

2.7. Wound-healing assay

Wound-healing assay were performed to evaluate cell migration capacity. After grown to confluence in 6-well plate, cells were incubated with 10 μg/ml mitomycin (Sigma, St. Louis, MO) for 1 h to inhibit cell proliferation, which could confound the evaluation of cell migration [26]. Wound was made through the monolayer cell with a 10 μl sterile pipette tip and cells were cultured with replaced medium. The percent of wound closure was calculated after 24 h and the assays were performed in three times.

2.8. Transwell invasion assay

For invasion assay, 24-well transwell chamber with 8-μm pore insert Corning Costar Corp, Corning, NY) was used. About 1×10^5 cells in 200 μL of serum-free medium were placed into the upper chamber coated with Matrigel (20 μl, BD Biosciences, Franklin Lakes, NJ), while serum containing medium was in the under chamber. After 24 h of incubation, cells on the upper side of the insert were removed carefully and cells adhering to the underside of the membrane were fixed in 20% methanol and stained with 0.1% crystal violet. The numbers of invaded cells were counted and each assay was performed in triplicate.

2.9. HCC mouse model

Orthotopic HCC model in mouse was established as described before [23]. Briefly, Stably transfected and luciferase labeled cells were subcutaneously injected into the left upper flanks of male nude mice (BALB/c, 4–6 weeks old). After two weeks, the subcutaneous tumors were resected and cut into pieces of approximately 1 mm^3 and implanted into the liver of nude mice (6 in each group). The tumor formation and metastasis were monitored by bioluminescence imaging using the Xenogen IVIS imaging system 100 (Caliper Lifescience, Hopkinton, MA). In brief, mice were injected intraperitoneally with D-luciferin (Caliper Lifescience, Hopkinton, MA) at 100 mg/kg and then subjected to imaging. The mice were sacrificed six weeks later and the livers and lungs were harvested, imaged and processed for histological examination. All animal experiments were performed at the Department of Laboratory Animals of CSU according to the guidelines approved by the Medical Experimental Animal Care Commission of CSU.

2.10. Immunofluorescence (IF)

Cells were fixed with 4% paraformaldehyde (PFA), permeabilized with 0.1% Triton X-100 and blocked with 5% bovine serum albumin (BSA). Then, cells were incubated with primary antibodies in PBST with 1% BSA overnight at 4 °C, followed by fluorescence labeled secondary antibody incubation for 30 min at room temperature. Actin cytoskeleton were stained with rhodamine-conjugated phalloidin (Roche, Basel, Switzerland) directly. DAPI was used for nuclear staining. Images were captured by inverted fluorescence microscope DMI4000-B (Leica, Wetzlar, Germany) and TCS SP8 confocal laser microscope (Leica, Wetzlar, Germany).

2.11. Gene set enrichment analysis

Gene Set Enrichment Analysis (GSEA) method was adopted to conduct Gene Ontology (GO) and Kyoto Encyclopedia of Genes and Genomes (KEGG) pathway analyses using The Cancer Genome Atlas database (TCGA, http://cancergenome.nih.gov). GSEA were performed with clusterProfiler package of *R* language and false discovery rate (FDR) < 0.25 and *P* < 0.05 were set as the cut-off criteria.

2.12. Multi-pathway Reporter Array

The Cignal Finder Cancer 10-Pathway Reporter Array (SABiosciences, Valencia, CA) including 10 most common and important pathways in cancer development was employed to investigate the potential pathways that were regulated by STMN2 in HCC. The assay was performed according to the manufacturer's instructions and done in triplicate. Relative firefly luciferase activity was calculated and normalized to the constitutively expressed renilla luciferase.

2.13. Immunoprecipitation (IP) assay

Cells were lysed in ice-cold RIPA buffer (CWBIO, Beijing, China) supplied with 1% protease inhibitor cocktail (CWBIO, Beijing, China). Lysate was centrifuged to remove insoluble fraction and subsequently cleared by incubation with protein G agarose (Cell Signaling Technology, Danvers, MA) for 1 h at 4 °C. The pre-cleared supernatant were incubated with primary antibodies or control IgG at 4 °C overnight. The immunocomplexes were next precipitated by incubation with protein G agarose (Cell Signaling Technology, Danvers, MA) for 2 h at 4 °C. The beads were washed with RIPA buffer five times and protein complexes were eluted out by 1 × SDS sample buffer and then subjected to western blot analysis.

2.14. Microtubule sedimentation assay

The Microtubule/Tubulin In Vivo Assay Biochem Kit (Cytoskeleton, Denver, CO) was used to isolate soluble and polymerized (cytoskeletal) tubulin according to the product manual. Briefly, cells were washed twice with 37°C PBS PH 7.4 and then lysed in microtubule stabilization buffer. Follwing a centrifugation at 14,000 rpm for 10 min at 37 °C, supernatants containing soluble tubulin were collected and pellets containing polymerized (cytoskeletal) tubulin were dissolved in a volume of microtubule depolymerization buffer equal to the lysate supernatant volume. The tubulin in supernatant and pellet fractions of the same volume were analyzed by western blot. The relative amounts of polymerized tubulin was evaluated by the ratio of densitometry value of polymerized tubulin to the sum of the densitometry values of soluble and polymerized tubulin [27].

2.15. Statistical analysis

Statistical analysis was performed using SPSS 18.0 software (SPSS Inc., Chicago, IL) and GraphPad Prism 6 (GraphPad Software, San Diego, CA). Data were presented as mean ± standard deviation (SD). Quantitative data were compared by student's *t*-test or Mann-Whitney *U* test when the variance is not homogeneous. Categorical data were analyzed using Chi-square test or Fisher exact test. Spearman's rank analysis was conducted to assess the correlations between different protein expressions. Survival curves were constructed using the Kaplan-Meier method and evaluated using log-rank test. Univariate and multivariate analyses were performed to determine prognostic factors based on the Cox proportional hazards regression model. *P* < 0.05 (two-tailed) was considered statistically significant.

3. Results

3.1. STMN2 expression is up-regulated in HCC tissues

Data sets from Oncomine database (https://www.oncomine.org) indicated that STMN2 mRNA was significantly up-regulated in HCC

tissues compared to normal liver tissues (NLTs) (Fig. 1A). By qRT-PCR detection in 30 pairs of frozen fresh HCC specimens, we found that STMN2 mRNA was markedly elevated in HCCs compared with matched ANLTs (Fig. 1B). Consistently, western blot further confirmed STMN2 up-regulation in HCC tissues at protein level (Fig. 1C). Then, we performed immunohistochemistry (IHC) to analyze STMN2 expression in two independent cohorts of HCCs and NLTs. The results showed that STMN2, mainly localized in the cytoplasm, was barely expressed in NLTs, but frequently elevated in HCCs (Fig. 1D). Of note, HCCs with early recurrence (≤2 years) (HCC-ER) showed much higher STMN2 expression than those without early recurrence (HCC-NR) (Fig. 1D).

DNA methylation is a common epigenetic mechanism of transcriptional regulation in HCC [28], and decreased methylation of gene promoter contributes to increased gene transcription [28,29]. Therefore, we further analyzed the promoter methylation status of STMN2 using TCGA-methylation database, and found that STMN2 promoter was hypomethylated in HCC tissues compared to normal liver tissues (Supplementary Fig. 1B). In line with it, the mRNA level of STMN2 was markedly increased in HCC samples of TCGA (Supplementary Fig. 1B). Altogether, these data fully indicated that STMN2 was up-regulated in HCC and this might be caused by promoter demethylation.

3.2. High STMN2 expression correlates with poor clinicopathological features and survival of HCC patients

We then investigated the clinical significance of STMN2 expression using two independent cohorts of HCC patients. STMN2 expression was defined as high and low according to the IHC scoring criteria mentioned in the materials and methods. In training cohort (n = 136), high expression of STMN2 was significantly associated with liver cirrhosis, advanced Edmondson-Steiner grade, macrovascular invasion (MaVI), microvascular invasion (MVI) and tumor early recurrence (all with $P <$ 0.05; Supplementary Table 2). Patients with high STMN2 expression suffered from shorter overall survival (OS) (1-, 3-, 5-year OS: 73.24%, 37.51%, 18.05% vs. 88.89%, 61.90%, 46.77%; $P < 0.001$) and worse disease-free survival (DFS) (1-, 3-, 5-year DFS: 57.75%, 27.14%, 15.27% vs. 76.56%, 53.99%, 36.07%; $P < 0.001$) than those with low STMN2 expression (Fig. 1E). Univariate and multivariate cox regression analysis indicated that STMN2 overexpression served as an independent risk factor for both OS (HR = 1.972, 95% CI: 1.262–3.081; $P = 0.003$) and DFS (HR = 1.634, 95% CI: 1.059–2.521; $P = 0.026$) (Table 1). The prognostic value of STMN2 expression was further verified in the validation cohort (n = 102, Supplementary Table 3). Collectively, these results indicated that STMN2 overexpression was associated with malignant behaviors and predicted poor prognosis of HCC.

3.3. STMN2 promotes HCC migration and invasion in vitro and metastasis in vivo

Similar to HCC tissues, STMN2 was also up-regulated in HCC cell lines compared with the normal liver cell line L02 according to qRT-PCR and western blot analyses (Fig. 2A and B). To determine the effect of STMN2 expression on the invasiveness of HCC cells, lowly metastatic potential cell lines PLC/PRF/5 and Huh7 with relatively low STMN2 expression and the highly metastatic potential cell lines HCCLM3 and MHCC97-H with high STMN2 expression were chosen for subsequent functional assays. We first stably raised STMN2 expression in PLC/PRF/5 and Huh7 cells and knocked down it by two independent shRNAs (shSTMN2-2 and shSTMN2-1) in HCCLM3 and MHCC97-H cells. Overexpression or knockdown efficiency was verified by qRT-PCR and western blot (Supplementary Fig. 2A). Wound-healing and transwell invasion assays showed that up-regulation of STMN2 in PLC/PRF/5 and Huh7 dramatically promoted cell migration and invasion compared with the control cells (Fig. 2C and Supplementary Fig. 2B). Conversely, STMN2 knockdown markedly inhibited the migratory and invasive capacities of HCCLM3 and MHCC97-H cells (Fig. 2C and Supplementary

Fig. 2B). To further assess the proinvasive role of STMN2 *in vivo*, orthotopic xenograft tumor models in nude mice were established. STMN2 expression in xenograft tumors was verified by IHC (Supplementary Fig. 2C). The results showed that STMN2 overexpression increased the incidence of pulmonary/intraheptatic metastasis and the number of pulmonary/intraheptatic metastasis nodule, whereas STMN2 knockdown reduced the incidence of pulmonary/intraheptatic metastasis and the number of pulmonary/intraheptatic metastasis nodule (Fig. 2D and E). In summary, STMN2 facilitated HCC cell migration and invasion *in vitro* as well as metastasis *in vivo*.

3.4. STMN2 induces EMT in HCC

In this study, we noticed that STMN2 overexpression enabled PLC/PRF/5 and Huh7 cells to change from round-like epithelial morphology to spindle-like mesenchymal appearance, whereas depletion of STMN2 in mesenchymal-like HCCLM3 and MHCC97-H cells led to a reverse effect (Fig. 3A and Supplementary Fig. 3A). These phenomenon together with the role of STMN2 in HCC invasion and metastasis, promoted us to determine whether STMN2 induced EMT in HCC. To this aim, gene set enrichment analysis (GSEA) was performed using the TCGA database and the result indicated that STMN2 was significantly correlated with EMT biological process in HCC (NES = 1.573, $P = 0.0001$, Supplementary Fig. 3B). Furthermore, western blot and qRT-PCR analyses showed that STMN2 overexpression in PLC/PRF/5 and Huh7 cells down-regulated epithelial markers (E-cadherin and β-catenin) and up-regulated mesenchymal markers expression (Vimentin, N-cadherin and Snail), whereas STMN2 knockdown increased epithelial markers and reduced mesenchymal markers expression in HCCLM3 and MHCC97-H cells (Fig. 3B and C and Supplementary Figs. 3C and D). Immunofluorescence (IF) detection of EMT markers in HCC cells also obtained similar results (Fig. 3D and Supplementary Fig. 3E). Moreover, IHC staining on consecutive sections showed that STMN2 was negatively associated with E-cadherin expression and positively correlated with Vimentin and Snail expression in HCC samples in both training and validation cohorts (Fig. 3E). Hence, it was concluded that STMN2 triggered EMT in HCC.

3.5. STMN2 activates TGFβ pathway in HCC

To unveil the functional mechanisms of STMN2 in HCC, we conducted GSEA analysis using the TCGA database to systemically screen the potential signaling pathways modulated by STMN2. The results showed that several term/pathways involved in cancer progression were significantly enriched, including Pathways in cancer, TGFβ pathway, Calcium pathway and MAPK pathway (Fig. 4. A, Supplementary Fig. 4). Moreover, a Cignal Finder Cancer 10-Pathway Reporter Array was performed in HCC cells and the results indicated that TGFβ signaling was the most significantly activated pathway upon STMN2 overexpression and vice versa (Fig. 4B). For the canonical TGFβ pathway (Smad-dependent), upon TGFβ binding to its receptors, Smad2/3 are recruited and phosphorylated at their C-terminal SSXS motif by TGFβ receptor type I (TβRI), subsequently forming a complex with Smad4 and translocating into nucleus for gene transcription [30]. To further confirm the influence of STMN2 expression on TGFβ pathway, western blot was performed to evaluate the activity of Smad2/3 in HCC cell lines after STMN2 gene interference. According to the results, the total expression of Smad2/3 showed no considerable changes, while the level of phosphorylated Smad2/3 (p-Smad2/3) was increased upon STMN2 overexpression in PLC/PRF/5 cells, and STMN2 knockdown in HCCLM3 cells decreased the level of p-Smad2/3 (Fig. 4C). Furthermore, IHC analysis showed that p-Smad2/3 expression was positively associated with STMN2 expression in HCC samples both in training and validation cohorts (Fig. 4D). These results indicated that STMN2 activated TGFβ signaling in HCC. In addition, somewhat surprisingly, we found that STMN2-induced TGFβ signaling activation in PLC/PRF/5^{STMN2} cells was
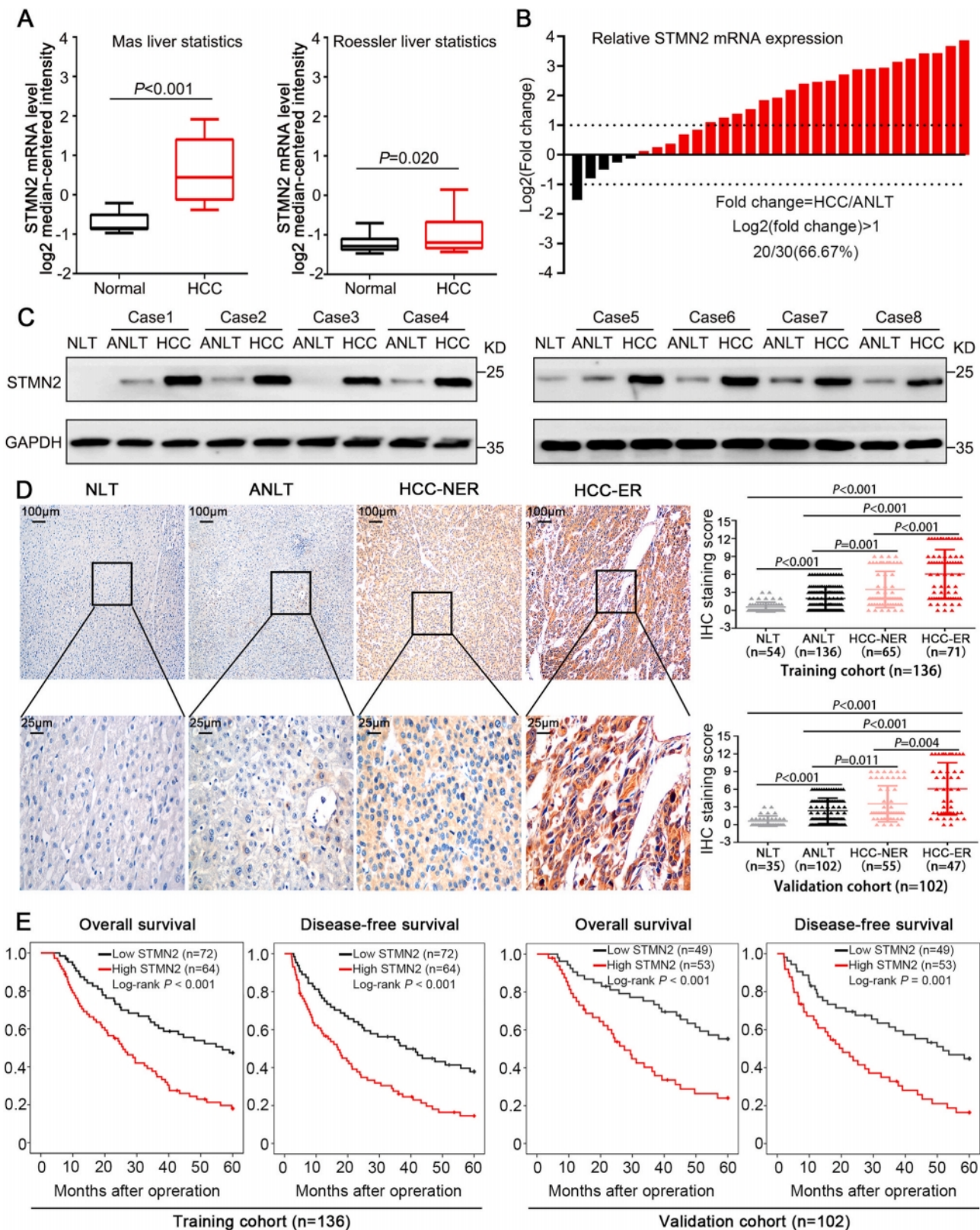
Fig. 1. STMN2 is up-regulated in HCC and predicts poor prognosis. (A) Comparing the level of STMN2 mRNA in HCC tissues and normal liver tissues in Oncomine database. (B) qRT-PCR analysis of STMN2 expression in thirty pairs of HCC samples. Data were presented as log2-fold change. (C) Western blot detected the expression of STMN2 in representative paired HCC samples and two normal liver tissues (NLT). (D) Representative IHC staining for STMN2 in NLT, adjacent nontumor liver tissue (ANLT), HCC without early tumor recurrence (HCC-NER) and HCC with early tumor recurrence (HCC-ER) (left panel). IHC staining score of STMN2 for NLT, ANLT, HCC-NER and HCC-ER in two independent cohorts (right panel). *P*-values were calculated by Mann-Whitney *U* test. (E) Overall survival (OS) and disease-free survival (DFS) of HCC patients with high or low STMN2 expression in training and validation cohorts (log-rank test).

Table 1

Univariate and multivariate analyses of risk factors associated with overall survival (OS) and disease-free survival (DFS) of HCC patients in training cohort.

Variables	OS				DFS			
	Univariate Analysis		Multivariate Analysis		Univariate Analysis		Multivariate Analysis	
	HR(95% CI)	*P* Value	HR(95% CI)	*P* Value	HR(95% CI)	*P* Value	HR(95% CI)	*P* Value
Gender								
Female	1				1			
Male	1.085(0.654–1.799)	0.753		NA	1.110(0.679–1.815)	0.676		NA
Age								
≤60 years	1				1			
>60 years	1.225(0.731–2.052)	0.441		NA	1.205(0.730–1.989)	0.466		NA
AFP								
≤20 ng/ml	1				1			
>20 ng/ml	1.292(0.827–2.016)	0.260		NA	1.418(0.918–2.190)	0.115		NA
HBsAg								
Negative	1				1			
Positive	1.307(0.795–2.149)	0.291		NA	1.459(0.892–2.386)	0.133		NA
Liver cirrhosis								
Absence	1		1		1			
Presence	1.633(1.023–2.067)	**0.040**	1.279(0.764–2.139)	0.349	1.294(0.841–1.992)	0.241		NA
Child-Pugh classification								
A	1				1			
B	1.473(0.879–2.468)	0.141		NA	1.336(0.801–2.229)	0.267		NA
Tumor nodule number								
Solitary	1				1			
Multiple (≥2)	1.553(0.998–2.417)	0.051		NA	1.450(0.945–2.223)	0.089		NA
Tumor size								
≤ 5 cm	1				1			
> 5 cm	1.508(0.985–2.308)	0.059		NA	1.412(0.940–2.120)	0.096		NA
Capsular formation								
Presence	1				1		1	
Absence	1.461(0.943–2.264)	0.090		NA	1.579(1.030–2.420)	**0.036**	0.996(0.635–1.560)	0.985
Edmondson-Steiner grade								
I&II	1		1		1		1	
III&IV	1.661(1.075–2.566)	**0.022**	1.486(0.915–2.413)	0.110	1.801(1.180–2.749)	**0.006**	1.516(0.971–2.367)	0.067
Macrovascular invasion								
Absence	1		1		1		1	
Presence	3.680(2.323–5.830)	**<0.001**	2.563(1.579–4.160)	**<0.001**	3.420(2.147–5.447)	**<0.001**	2.442(1.502–3.968)	**<0.001**
Microvascular invasion								
Absence	1		1		1		1	
Presence	2.341(1.539–3.559)	**<0.001**	2.014(1.307–3.102)	**0.002**	2.290(1.590–3.428)	**<0.001**	1.856(1.209–2.847)	**0.005**
BCLC stage								
0&A	1		1		1		1	
B&C	1.685(1.072–2.646)	**0.024**	1.393(0.683–2.188)	0.377	1.704(1.104–2.629)	**0.016**	1.438(0.740–2.252)	0.262
TNM stage								
I	1		1		1		1	
II&III	3.059(1.722–5.432)	**<0.001**	1.899(1.035–3.483)	**0.038**	1.837(1.669–4.821)	**<0.001**	1.988(1.129–3.500)	**0.017**
STMN2 expression								
Low	1		1		1		1	
High	2.306(1.498–3.549)	**<0.001**	1.972(1.262–3.081)	**0.003**	2.044(1.358–3.076)	**0.001**	1.634(1.059–2.521)	**0.026**

Abbreviations: AFP, alpha-fetoprotein; HBsAg, hepatitis B surface antigen; TNM, tumor node metastasis; BCLC, Barcelona Clinic Liver Cancer. HR, hazard risk ratio; CI, confidence interval; NA, not applicable.

not much attenuated by TGFβ signaling inhibitor SB431542 even at a high drug concentration (2 μM) [31,32], which was enough to effectively block the interaction between TGFβ and TβRI, thus abolishing TGFβ stimulation on this pathway. Similarly, HCCLM3^{shCtrl} still maintained a certain level of p-Smad2/3 after SB431542 treatment (Fig. 4E), which was further verified in two other HCC cell lines (MHCC97-H and HepG2) with high endogenous expression of STMN2 (Supplementary Fig. 4B). These findings suggested that STMN2 could enhance TGFβ signaling even independent of TGFβ stimulation, at least to some extent.

3.6. STMN2 induces EMT via TGFβ pathway

Considering the essential role of TGFβ pathway in EMT [5], we next determined whether STMN2 induced EMT in HCC via this pathway. Since Smad2/3 are key intracellular transducers for TGFβ signaling [30], we simultaneously knocked down Smad2/3 to block TGFβ pathway in corresponding HCC cells (Supplementary Fig. 5A). Expectedly, Smad2/3 knockdown effectively inhibited TGFβ signaling and reversed the expression of downstream EMT markers in STMN2-overexpressing cells

(PLC/PRF/5^{STMN2} and HCCLM3^{shCtrl}) (Fig. 5A). However, PLC/PRF/5^{Ctrl} and HCCLM3$^{shSTMN2-2}$ cells with low level of STMN2 had low activity of TGFβ signaling and deletion of Smad2/3 in these cells only exerted marginal effect on the expression of EMT markers (Fig. 5A). These results were further confirmed by IF and qRT-PCR analyses (Fig. 5B, Supplementary Fig. 5B). Consistently, Smad2/3 knockdown effectively blocked STMN2-induced cell migration and invasion (Fig. 5C and D and Supplementary Figs. 5C and D). Moreover, consecutive sections of xenograft tumors were subjected to IHC analysis, indicating that p-Smad2/3, Vimentin and Snail expression were increased and E-cadherin expression was decreased in STMN2-overexpressing tumors compared with the controls, whereas opposite results were observed in STMN2-knockdown tumors (Fig. 5E). Together, these data further reinforced the link between STMN2 and TGFβ pathway, and fully demonstrated that STMN2 induced EMT via this pathway in HCC.
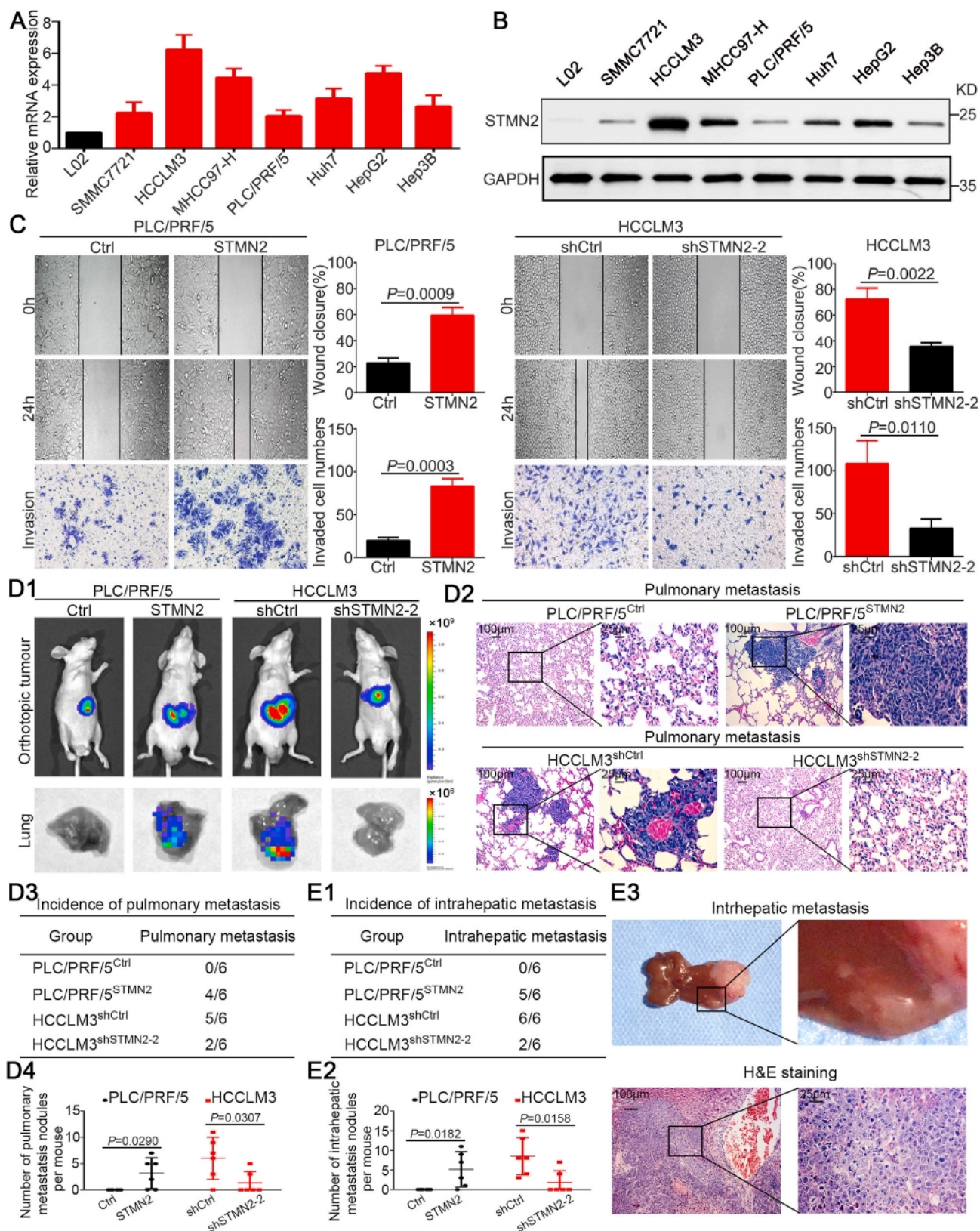
Fig. 2. STMN2 promotes HCC cell migration, invasion and metastasis *in vitro* and *in vivo*. STMN2 expression in normal liver cell line (L02) and seven HCC cell lines was analyzed by qRT-PCR (A) and Western blot (B). (C) The effects of STMN2 overexpression or knockdown on cell migratory and invasive capacity were evaluated by wound-healing assay and transwell invasion assay respectively. (D1) Representative bioluminescent images of orthotopic xenograft tumor and pulmonary metastasis; (D2) Histological analyses of pulmonary metastatic nodules by H&E staining and typical images were shown; (D3) The incidence of pulmonary metastasis and (D4) the number of pulmonary metastasis nodule in each group. (E1) The incidence of intrahepatic metastasis and (E2) the number of intrahepatic metastasis nodule in different groups; (E3) Representative images of intrahepatic metastasis. Six mice per group. Data were compared by student's *t*-test. Abbreviation: H&E, hematoxylin and eosin.
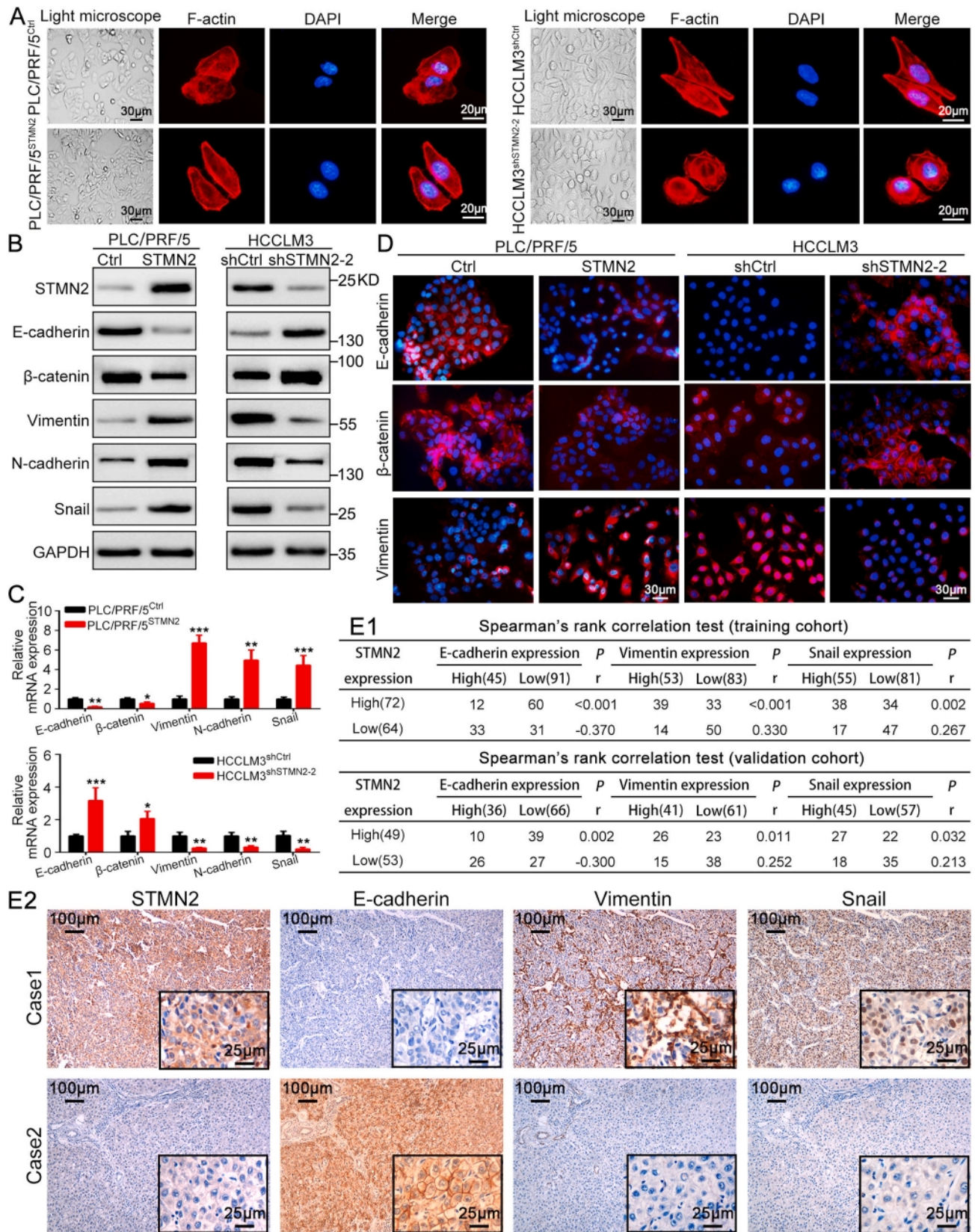
Spearman's rank correlation test (training cohort)

STMN2 expression	E-cadherin expression		P	Vimentin expression		P	Snail expression		P
	High(45)	Low(91)	r	High(53)	Low(83)	r	High(55)	Low(81)	r
High(72)	12	60	<0.001	39	33	<0.001	38	34	0.002
Low(64)	33	31	-0.370	14	50	0.330	17	47	0.267

Spearman's rank correlation test (validation cohort)

STMN2 expression	E-cadherin expression		P	Vimentin expression		P	Snail expression		P
	High(36)	Low(66)	r	High(41)	Low(61)	r	High(45)	Low(57)	r
High(49)	10	39	0.002	26	23	0.011	27	22	0.032
Low(53)	26	27	-0.300	15	38	0.252	18	35	0.213

Fig. 3. STMN2 induces EMT in HCC. (A) Light microscopy and immunofluorescence (IF) staining of cytoskeleton showed morphological changes of indicated cells. Nuclei was stained with DAPI (blue), and cytoskeleton was visualized by actin staining using rhodamine-phalloidin (red). (B) Western blot, (C) qRT-PCR and (D) IF detected the expression of EMT markers in STMN2-interfered and control cells. Data of experimental groups were normalized to corresponding control groups (*$P <$ 0.05, **$P < 0.01$ and ***$P < 0.001$; student's *t*-test). (E1) Correlations between STMN2 and EMT markers expression in HCC samples were analyzed by spearman's rank test. (E2) Representative IHC images of STMN2 and EMT markers expression in serial sections of HCC specimens.
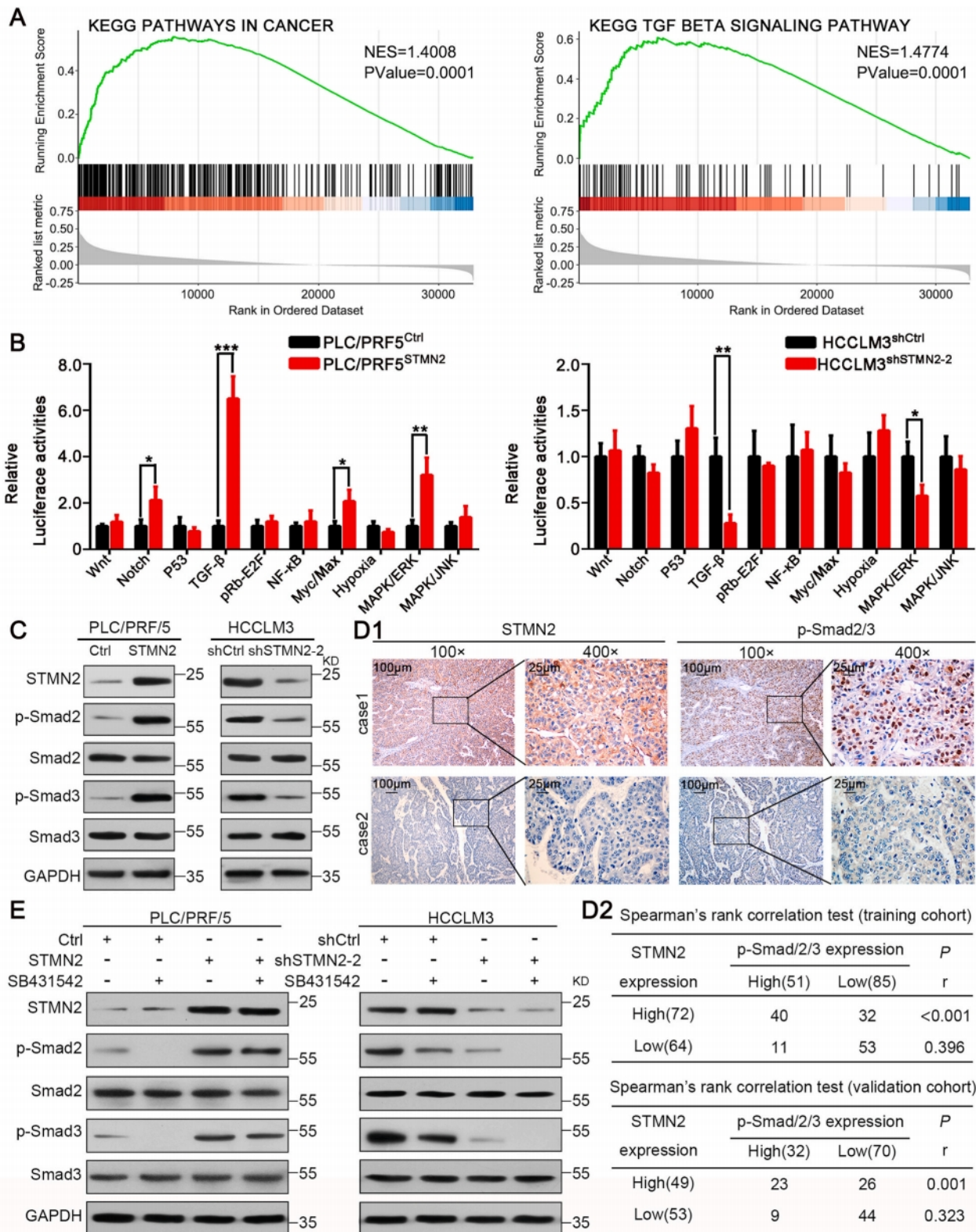
Fig. 4. STMN2 activates TGFβ pathway in HCC. (A) GSEA-based KEGG pathway analysis for STMN2 using TCGA database. GESA plots showed the significant enriched pathways. (B) Cancer 10-pathway Reporter Array showed the pathway alterations in HCC cells after STMN2 expression interference, (*$P < 0.05$, **$P < 0.01$, ***$P < 0.001$; student's *t*-test). (C) Key effectors of TGFβ signaling were examined by western blot in indicated cells. (D1) IHC staining of STMN2 and p-Smad2/3 in consecutive sections of representative HCC cases; (D2) The correlation between STMN2 and p-Smad2/3 expression in HCC samples was analyzed in training and validation cohorts using Spearman's rank test. (E) Western blot analysis of key effectors of TGFβ signaling in STMN2-interfered cells with or without SB431542 (2 μM) treatment. Abbreviations: GSEA, Gene set enrichment analysis; KEGG, Kyoto Encyclopedia of Genes and Genomes; TCGA, The Cancer Genome Atlas.
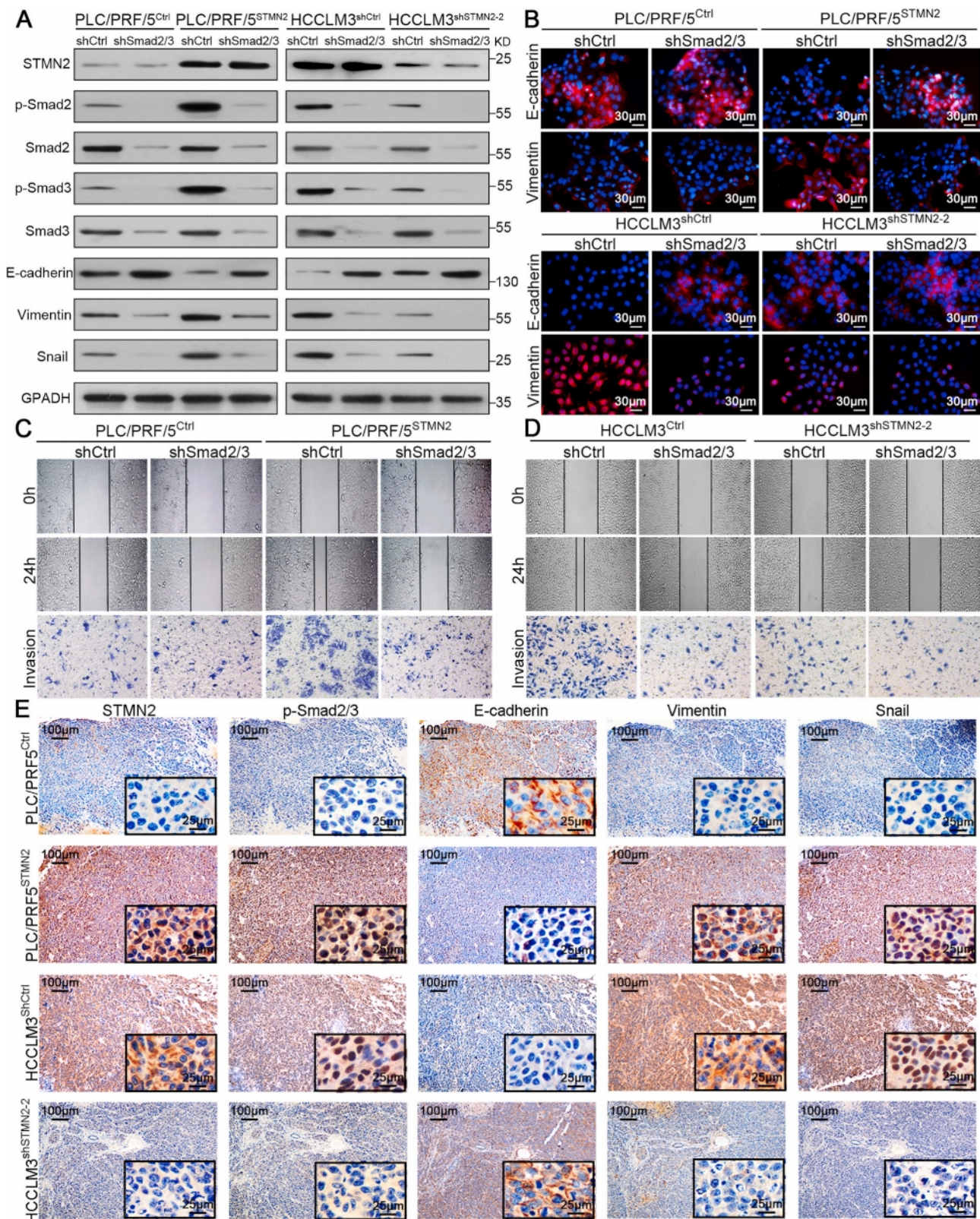
Fig. 5. STMN2 promotes EMT via TGFβ pathway. Blocking TGFβ pathway by simultaneously knocking down Smad2/3 in STMN2-interfered cells or control cells. Western blot (A) and IF (B) analyzed the expression of EMT markers. Wound-healing assay (C) and transwell invasion assay (D) examined the migratory and invasive capacities of indicated cells. (E) Representative IHC images of STMN2, p-Smad2/3 and EMT markers staining in serial sections of orthotopic xenograft tumors generated from PLC/PRF/5^Ctrl, PLC/PRF/5^STMN2, HCCLM3^shCtrl and HCCLM3^shSTMN2-2 cells.

3.7. STMN2 facilitates samd2/3 release and activation by orchestrating microtubule disassembly

We then investigated how STMN2 activates TGFβ pathway in HCC. Smad2/3 were found to bind microtubules (MTs) in epithelial cells and MTs negatively regulated TGFβ pathway by tethering Smad2/3 in the MT cytoskeleton network, which prevented Samd2/3 access to and phosphorylation by TGFβ-activated TβRI [33]. Since STMN2 is a predominant MT-destabilizing factor, we speculated that STMN2 might facilitate Smad2/3 release and activation by modulating MTs disassembly. To test this hypothesis, we first examined the effect of STMN2 on MTs in HCC cells. Results showed that the level of acetylated-α-tubulin, a known marker of stable and long-lived MT [34], was decreased after STMN2 overexpression in PLC/PRF/5 cells, whereas STMN2 knockdown increased it in HCCLM3 cells according to western blot and IF analyses (Fig. 6. A1, 2 and Supplementary Fig. 6A). Consistently, STMN2 overexpression increased soluble dimeric tubulin and decreased polymerized tubulin, whereas STMN2 knockdown obtained inverse results, as evaluated by the microtubule sedimentation assay (Fig. 6A3. IF staining of MT also showed that there was a reduction of MT intensity in PLC/PRF/5^{STMN2} and HCCLM3^{shCtrl} cells compared with PLC/PRF/5^{Ctrl} and HCCLM3$^{shSTMN2-2}$ cells respectively (Fig. 6B and Supplementary Fig. 6B). Collectively, these data indicated that STMN2 decreased MT stability and promoted MTs disassembly in HCC.

Next, we tested the association between Smad2/3 and MTs in HCC. Smad2/3 are mainly localized in cytoplasm, which will rapidly translocate into nuclear to regulate gene transcription after phosphorylation [30]. In this study, we observed that Smad2/3 co-localized with MTs in cell cytoplasm (Fig. 6B and Supplementary Fig. 6C). This phenomenon was further confirmed by immunoprecipitation (IP) examination, which showed that Smad2/3 bound tubulin in HCC cells (Fig. 6C). These results were consistent with the previous report showing that endogenous Smad2/3 bound MTs in epithelial cells [33].

Further, we revealed that STMN2 overexpression impaired the binding of Smad2/3 to MT and vice versa (Fig. 6C). Consistently, up-regulation of STMN2 in PLC/PRF/5 cells resulted in a decrease of MT density and notable increase of Smad2/3 release and nuclear translocation, whereas, after STMN2 depletion in HCCLM3 cells, MT amount was increased and more Samd2/3 were trapped in the MT network and less translocated into nuclear (Fig. 6B and Supplementary Figs. 6B and C). Cell fractionation analysis by western blot also showed that STMN2 overexpression, not affecting the total smad2/3 level, substantially decreased cytoplastic smad2/3 and increased nuclear smad2/3 and vice versa (Supplementary Fig. 6D). Furthermore, cells were treated with MT-stabilizing agent taxol (1 μM) [33] to verify that STMN2-induced Smad2/3 activation was indeed dependent on its MT-destabilizing activity. The efficiency of taxol in stabilizing MT in STMN2-interfered cells was confirmed before subsequent experiments (Supplementary Fig. 6E). Expectedly, taxol prevented Smad2/3 dissociation from MTs (Fig. 6D) and inhibited its phosphorylation and transcriptional regulation on downstream EMT markers in STMN2-overexpressing cells (Fig. 6E), but had no considerable effect in low STMN2-expressing cells, which contained stable MT networks (Fig. 6D and E). IF and qRT-PCR assays also showed that taxol reversed the EMT process caused by STMN2 over-expression (Fig. 6F and Supplementary Fig. 6F). Consistently, STMN2-mediated cell migration and invasion were effectively inhibited by taxol treatment (Supplementary Fig. 6G). Altogether, these results indicated that STMN2 disrupted the complexes between smad2/3 and MTs, and promoted Smad2/3 release, phosphorylation and nuclear translocation via modulating MTs disassembly, thus facilitating TGFβ signaling and EMT.

3.8. TTK mediates STMN2-induced phosphorylation of Smad2/3

We then attempted to explore the mechanisms underlying TGFβ-independent phosphorylation of Smad2/3 caused by STMN2 overexpression, as STMN2 did not have phosphatase activity itself. Interestingly, a previous study suggested that MT disassembly enhanced TTK (also named Mps1) expression and TTK could directly mediate TGFβ-independent phosphorylation of Smad2/3 [35]. Moreover, TTK was dysregulated in various cancers including HCC [36,37], and play a important role in cancer invasion and EMT [36,38]. These evidences raised the possibility that TTK would be implicated in STMN2-induced phosphorylation of Smad2/3 in HCC. To this end, we first tested the effect of STMN2 expression on TTK activity. The results showed that STMN2 overexpression in PLC/PRF/5 cells increased TTK expression and STMN2 knockdown decreased it in HCCLM3 cells (Supplementary Fig. 6H), and STMN2-induced TTK expression could be blocked by taxol (1 μM) treatment (Supplementary Fig. 6H), suggesting that STMN2 promoted TTK expression in a MT-destabilizing manner. Further, knockdown of TTK in PLC/PRF/5^{STMN2} and HCCLM3^{shCtrl} cells could effectively inhibit the expression of p-Smad2/3 induced by STMN2 (Fig. 6G), indicating that TTK was responsible for STMN2-induced phosphorylation of Smad2/3 in HCC.

4. Discussion

MT is a highly dynamic polymer and cells can adapt their MT cytoskeleton to perform different biological functions by modulating MT dynamics [9]. Accumulating evidences suggest that cancer invasion is associated with aberrant MT dynamics and MT dynamics regulators are frequently found to be dysregulated in malignancies [19,20,39,40]. STMN2, as a MT destabilizer, plays a crucial role in regulating MT dynamics [12,13] and cell motility [15,16]. Previously, a study suggested that activation of β-catenin/TCF could promote STMN2 expression in hepatoma cells [41]. Besides, STMN2 was found to be implicated in PAK4-induced gastric cancer invasion [42]. It has been shown more recently that STMN2 overexpression predicts poor survival in non-small-cell lung cancer [43] and ovarian cancer [44]. Beyond that, the significance of STMN2 in cancers remains elusive.

Herein, we found that STMN2 is barely expressed in normal liver tissues, which is consistent with the previous study [15], but markedly up-regulated in HCC tissues. Meanwhile, according to TCGA-methylation database analysis, its up-regulation may be caused by promoter demethylation, which together with the mechanisms underlying STMN2 promoter demethylation deserve further investigation. In addition, we revealed that HCC patients with early recurrence show significantly higher STMN2 expression than those without early recurrence, implying the potential of STMN2 to determine metastatic behavior [45]. Furthermore, we found that STMN2 overexpression is correlated with aggressive clinicopathological features and HCC patients with high STMN2 expression suffered from shorter OS and DFS. In line with clinical observations, functional assays demonstrated that STMN2 promotes HCC cell migration, invasion and metastasis *in vitro* and *in vivo*. Recently, a few emerging evidences have suggested that EMT, a key process in cancer invasion [3], is associated with aberrant MT dynamics and MT-destabilizing factors may contribute to EMT [18–20]. Consistently, in this study, we demonstrated that STMN2 triggers EMT. Together, these results suggest that STMN2 is an oncogene and plays an crucial role in HCC metastasis.

Canonical TGFβ pathway (Smad-dependent) is the major inducer of EMT and plays a predominant role in cancer cells dissemination and metastasis [3,5]. Hyperactivation of TGF-β pathway is a common event and also a hallmark of aggressive HCC [30,32]. Here, we found that STMN2 could significantly enhance TGFβ pathway in HCC. Blocking TGFβ signaling by deleting Smad2/3 in HCC cells significantly abolished STMN2-mediated EMT, migration and invasion, suggesting that STMN2 induces EMT and metastasis via TGFβ pathway in HCC.

Next, we wondered how STMN2 activates TGFβ pathway. It has been well-established that MT plays a critical role in intracellular signals transduction through several mechanisms, such as regulating the availability of signaling molecules by sequestering and releasing means
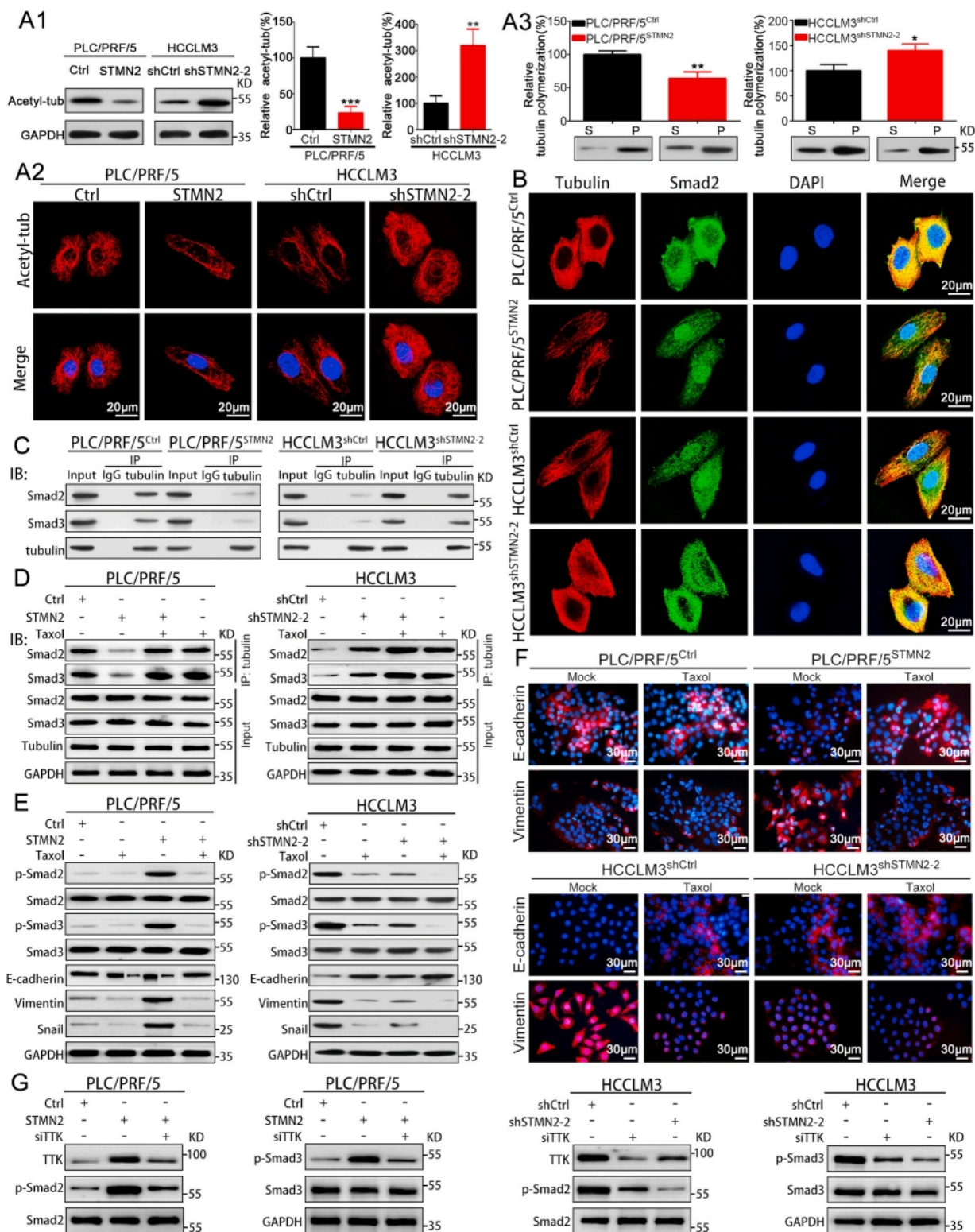
Fig. 6. STMN2 facilitates samd2/3 release and activation by orchestrating microtubule disassembly. (A1) Acetylated-α-tubulin (acetyl-tub) was examined by western blot and bands were subjected to densitometry analysis. Values were normalized to those in corresponding control cells. (A2) Cells were stained with acetyl-tub antibody and analyzed by immunofluorescence (IF). (A3) Soluble (S) and polymerized (P) tubulin in indicated cells were detected by western blot. The bands were subjected to densitometry analysis and the percentage of polymerized tubulin in STMN2-interfered cells was normalized to that in corresponding control cells. (B) Representative confocal images of co-immunofluorescent staining of Smad2 (green) and MTs (red) in indicated cells. (C) Immunoprecipitation (IP) analysis of the interactions between Smad2/3 and tubulin in indicated cells. (D) IP analysis of the interactions between Smad2/3 and tubulin in indicated cells with or without taxol (1 μM) treatment. (E) Western blot examined the expression of p-Smad2, p-Smad3, Smad2, Smad3 and EMT markers in STMN2-interfered cells and the control cells in the presence or absence of taxol (1 μM). STMN2-interfered cells and the control cells were treated with taxol (1 μM) or DMSO (Mock) and then subjected to IF detection of EMT markers (F). *$P < 0.05$, **$P < 0.01$, ***$P < 0.001$; *P*-values were calculated by Student's *t*-test. (G) Western blot analysis of the expression of p-Smad2, p-Smad3, Smad2 and Smad3 in STMN2-interfered cells with or without TTK knockdown.

[10,33]. In the current study, we found that STMN2 mediates MTs disassembly, disrupts MT-Smad complex, and release Smad2/3 from the MT network, consequently facilitating Samd2/3 access to and phosphorylation by TGFβ-activated TβRI [30,33], consequently enhancing TGFβ pathway. Interestingly, we further found that, via modulating MT disassembly, STMN2 could enhance TTK expression, a protein kinase could directly phosphorylate Smad2/3 [35], and thus induced TGFβ-independent Smad2/3 phosphorylation. This is in line with previous studies that had also showed TGFβ-independent Smad2/3 phosphorylation following MTs disruption [33,35,46]. Above all, these results indicate that STMN2 enhances TGFβ pathway in both TGFβ-dependent and -independent manners via modulating MTs disassembly, thereby triggering EMT, which for the first time links the MT cytoskeleton to smad2/3 activity in HCC and broadens our understanding of the activation of TGFβ pathway in this type of cancer. Generally, tumor fate is governed by the cell autonomous properties and microenvironmental cues [47,48]. TGFβ has emerged as a major microenviromental cue in favor of HCC progression [47,48]. In addition to the basal level of TGFβ secreted by tumor cell themselves, elevated TGFβ by tumor microenviroment plays a prominent role in HCC invasion and metastasis [30, 48]. Theoretically, during the process of metastasis, by virtue of STMN2-MT-Smads axis, HCC cells may adapt themselves to insufficient TGFβ stimulation in the changing microenvironment so as to facilitate EMT and metastasis efficiently. Nowadays, inhibiting TGFβ pathway represents a promising approach to combat HCC progression [49]. However, current strategies targeting TGFβ signaling mainly focus on the TGFβ-TβR axis [49,50]. According to our results, targeting STMN2-MT-Smads axis may be also important to effectively block TGFβ signaling in HCC with high STMN2 expression.

Moreover, in contrast to the traditional notion that intracellular signaling pathways regulate cytoskeleton rearrangement to induce EMT [5,7], we here demonstrated that MT cytoskeleton rearrangement could inversely regulate TGFβ signaling to facilitate EMT, providing the first evidence concerning the significance of MT dynamics for EMT in HCC and shedding new light on how MT dynamics contribute to this process. MTs and their dynamics are attractive therapeutic targets in various cancers including HCC [51–54]. However, conventional MT-targeting agents, which directly target MT itself, is limitedly used in HCC due to side effects and chemoresistance [51,54]. Interfering MT dynamics is the main mechanism of action of blocking MT-related oncogenic effects [51], and increasing evidences highlight that tumor-specific MT dynamics regulators are promising targets for developing new anticancer agents with improved specificity, enhanced efficacy and reduced toxicity [51,55–57]. Our results also provide rationale for targeting MT dynamics regulator and support the potential utility of STMN2 as a target for developing novel therapeutic strategies to combat HCC metastasis.

In summary, we revealed that STMN2 is up-regulated in HCC and associated with early recurrence and worse survival. STMN2 coordinates MT cytoskeleton rearrangement and TGFβ signaling to facilitate EMT and metastasis, extending our understanding of the molecular mechanism underlying HCC metastasis. STMN2 could serve as a promising prognostic biomarker and potential therapeutic target for HCC.

Ethics approval and consent to participant

This study was approved by the Ethics Committee of Xiangya Hospital of Central South University and The Affiliated Cancer Hospital of Xiangya School of Medicine. Written informed consent was obtained from each patient enrolled in this study. Animal experiments were approved by the Institutional Animal Care and Use Committee of Central South University.

Financial Support

This work was supported by the National Science and Technology

CRediT authorship contribution statement

Fang-Jing Zhong: Data curation, Formal analysis, Writing – original draft, Writing – review & editing, wrote the manuscript, analyzed and interpreted data, conducted bioinformatic analysis, conceived and designed this project, performed experiments. **Bo Sun:** Data curation, Formal analysis, Writing – original draft, Writing – review & editing, analyzed and interpreted data, performed experiments. **Mo-Mo Cao:** Data curation, Formal analysis, Writing – original draft, Writing – review & editing, analyzed and interpreted data, performed experiments. **Cong Xu:** Data curation, Formal analysis, Writing – original draft, Writing – review & editing, analyzed and interpreted data, performed experiments. **Yi-Ming Li:** Data curation, Formal analysis, Writing – original draft, Writing – review & editing, analyzed and interpreted data, conducted bioinformatic analysis. **Lian-Yue Yang:** Data curation, Formal analysis, Writing – original draft, Writing – review & editing, revised the manuscript, analyzed and interpreted data, conceived and designed this project.

Declaration of competing interest

The authors declare that they have no known competing financial interests or personal relationships that could have appeared to influence the work reported in this paper.

Acknowledgements

Appendix A. Supplementary data

Supplementary data to this article can be found online at https://doi.org/10.1016/j.canlet.2021.03.001.

References

[1] F. Bray, J. Ferlay, I. Soerjomataram, R.L. Siegel, L.A. Torre, A. Jemal, Global cancer statistics 2018: GLOBOCAN estimates of incidence and mortality worldwide for 36 cancers in 185 countries, Ca - Cancer J. Clin. 68 (2018) 394–424.

[2] A. Forner, M. Reig, J. Bruix, Hepatocellular carcinoma, Lancet 391 (2018) 1301–1314.

[3] V. Mittal, Epithelial mesenchymal transition in tumor metastasis, Annu. Rev. Pathol. 13 (2018) 395–412.

[4] G. Giannelli, P. Koudelkova, F. Dituri, W. Mikulits, Role of epithelial to mesenchymal transition in hepatocellular carcinoma, J. Hepatol. 65 (2016) 798–808.

[5] S. Lamouille, J. Xu, R. Derynck, Molecular mechanisms of epithelial-mesenchymal transition, Nat. Rev. Mol. Cell Biol. 15 (2014) 178–196.

[6] M. Dogterom, G.H. Koenderink, Actin-microtubule crosstalk in cell biology, Nat. Rev. Mol. Cell Biol. 20 (2019) 38–54.

[7] M. Yilmaz, G. Christofori, EMT, the cytoskeleton, and cancer cell invasion, Canc. Metastasis Rev. 28 (2009) 15–33.

[8] H.T. Morris, L.M. Machesky, Actin cytoskeletal control during epithelial to mesenchymal transition: focus on the pancreas and intestinal tract, Br. J. Canc. 112 (2015) 613–620.

[9] A. Desai, T.J. Mitchison, Microtubule polymerization dynamics, Annu. Rev. Cell Dev. Biol. 13 (1997) 83–117.

[10] G.G. Gundersen, T.A. Cook, Microtubules and signal transduction, Curr. Opin. Cell Biol. 11 (1999) 81–94.

[11] L. Cassimeris, The oncoprotein 18/stathmin family of microtubule destabilizers, Curr. Opin. Cell Biol. 14 (2002) 18–24.

[12] C. Conde, A. Caceres, Microtubule assembly, organization and dynamics in axons and dendrites, Nat. Rev. Neurosci. 10 (2009) 319–332.

[13] B.M. Riederer, V. Pellier, B. Antonsson, G. Di Paolo, S.A. Stimpson, R. Lutjens, S. Catsicas, G. Grenningloh, Regulation of microtubule dynamics by the neuronal growth-associated protein SCG10, Proc. Natl. Acad. Sci. U. S. A. 94 (1997) 741–745.

[14] I. Bieche, A. Maucuer, I. Laurendeau, S. Lachkar, A.J. Spano, A. Frankfurter, P. Levy, V. Manceau, A. Sobel, M. Vidaud, P.A. Curmi, Expression of stathmin family genes in human tissues: non-neural-restricted expression for SCLIP, Genomics 81 (2003) 400–410.

[15] V. Paradis, D. Dargere, Y. Bieche, T. Asselah, P. Marcellin, M. Vidaud, P. Bedossa, SCG10 expression on activation of hepatic stellate cells promotes cell motility through interference with microtubules, Am. J. Pathol. 177 (2010) 1791–1797.

[16] N. Westerlund, J. Zdrojewska, A. Padzik, E. Komulainen, B. Bjorkblom, E. Rannikko, T. Tararuk, C. Garcia-Frigola, J. Sandholm, L. Nguyen, T. Kallunki, M. J. Courtney, E.T. Coffey, Phosphorylation of SCG10/stathmin-2 determines multipolar stage exit and neuronal migration rate, Nat. Neurosci. 14 (2011) 305–313.

[17] H.Y. Yue, C. Yin, J.L. Hou, X. Zeng, Y.X. Chen, W. Zhong, P.F. Hu, X. Deng, Y. X. Tan, J.P. Zhang, B.F. Ning, J. Shi, X. Zhang, H.Y. Wang, Y. Lin, W.F. Xie, Hepatocyte nuclear factor 4alpha attenuates hepatic fibrosis in rats, Gut 59 (2010) 236–246.

[18] Y. Nakaya, E.W. Sukowati, Y. Wu, G. Sheng, RhoA and microtubule dynamics control cell-basement membrane interaction in EMT during gastrulation, Nat. Cell Biol. 10 (2008) 765–775.

[19] N. Li, P. Jiang, W. Du, Z. Wu, C. Li, M. Qiao, X. Yang, M. Wu, Siva1 suppresses epithelial-mesenchymal transition and metastasis of tumor cells by inhibiting stathmin and stabilizing microtubules, Proc. Natl. Acad. Sci. U. S. A. 108 (2011) 12851–12856.

[20] J. Wu, Z. He, X.M. Yang, K.L. Li, D.L. Wang, F.L. Sun, RCCD1 depletion attenuates TGF-beta-induced EMT and cell migration by stabilizing cytoskeletal microtubules in NSCLC cells, Canc. Lett. 400 (2017) 18–29.

[21] S. Xiao, R.M. Chang, M.Y. Yang, X. Lei, X. Liu, W.B. Gao, J.L. Xiao, L.Y. Yang, Actin-like 6A predicts poor prognosis of hepatocellular carcinoma and promotes metastasis and epithelial-mesenchymal transition, Hepatology 63 (2016) 1256–1271.

[22] D.G. Altman, L.M. McShane, W. Sauerbrei, S.E. Taube, Reporting recommendations for tumor marker prognostic studies (REMARK): explanation and elaboration, BMC Med. 10 (2012) 51.

[23] R.M. Chang, H. Yang, F. Fang, J.F. Xu, L.Y. Yang, MicroRNA-331-3p promotes proliferation and metastasis of hepatocellular carcinoma by targeting PH domain and leucine-rich repeat protein phosphatase, Hepatology 60 (2014) 1251–1263.

[24] Y. Wang, F. Bu, C. Royer, S. Serres, J.R. Larkin, M.S. Soto, N.R. Sibson, V. Salter, F. Fritzsche, C. Turnquist, S. Koch, J. Zak, S. Zhong, G. Wu, A. Liang, P.A. Olofsen, H. Moch, D.C. Hancock, J. Downward, R.D. Goldin, J. Zhao, X. Tong, Y. Guo, X. Lu, ASPP2 controls epithelial plasticity and inhibits metastasis through beta-catenin-dependent regulation of ZEB1, Nat. Cell Biol. 16 (2014) 1092–1104.

[25] X. Lin, X. Duan, Y.Y. Liang, Y. Su, K.H. Wrighton, J. Long, M. Hu, C.M. Davis, J. Wang, F.C. Brunicardi, Y. Shi, Y.G. Chen, A. Meng, X.H. Feng, PPM1A functions as a Smad phosphatase to terminate TGFbeta signaling, Cell 125 (2006) 915–928.

[26] C.E. Pullar, J. Chen, R.R. Isseroff, PP2A activation by beta2-adrenergic receptor agonists: novel regulatory mechanism of keratinocyte migration, J. Biol. Chem. 278 (2003) 22555–22562.

[27] G.N. Alesi, L. Jin, D. Li, K.R. Magliocca, Y. Kang, Z.G. Chen, D.M. Shin, F.R. Khuri, S. Kang, RSK2 signals through stathmin to promote microtubule dynamics and tumor metastasis, Oncogene 35 (2016) 5412–5421.

[28] I.P. Pogribny, I. Rusyn, Role of epigenetic aberrations in the development and progression of human hepatocellular carcinoma, Canc. Lett. 342 (2014) 223–230.

[29] E.M. Michalak, M.L. Burr, A.J. Bannister, M.A. Dawson, The roles of DNA, RNA and histone methylation in ageing and cancer, Nat. Rev. Mol. Cell Biol. 20 (2019) 573–589.

[30] G. Giannelli, E. Villa, M. Lahn, Transforming growth factor-beta as a therapeutic target in hepatocellular carcinoma, Canc. Res. 74 (2014) 1890–1894.

[31] J.N. Zhou, Q. Zeng, H.Y. Wang, B. Zhang, S.T. Li, X. Nan, N. Cao, C.J. Fu, X.L. Yan, Y.L. Jia, J.X. Wang, A.H. Zhao, Z.W. Li, Y.H. Li, X.Y. Xie, X.M. Zhang, Y. Dong, Y. C. Xu, L.J. He, W. Yue, X.T. Pei, MicroRNA-125b attenuates epithelial-mesenchymal transitions and targets stem-like liver cancer cells through small mothers against decapentaplegic 2 and 4, Hepatology 62 (2015) 801–815.

[32] H. Sun, Z. Peng, H. Tang, D. Xie, Z. Jia, L. Zhong, S. Zhao, Z. Ma, Y. Gao, L. Zeng, R. Luo, K. Xie, Loss of KLF4 and consequential downregulation of Smad7 exacerbate oncogenic TGF-beta signaling in and promote progression of hepatocellular carcinoma, Oncogene 36 (2017) 2957–2968.

[33] C. Dong, Z. Li, R.J. Alvarez, X.H. Feng, P.J. Goldschmidt-Clermont, Microtubule binding to Smads may regulate TGF beta activity, Mol. Cell 5 (2000) 27–34.

[34] A. Szyk, A.M. Deaconescu, J. Spector, B. Goodman, M.L. Valenstein, N. E. Ziolkowska, V. Kormendi, N. Grigorieff, A. Roll-Mecak, Molecular basis for age-dependent microtubule acetylation by tubulin acetyltransferase, Cell 157 (2014) 1405–1415.

[35] S. Zhu, W. Wang, D.C. Clarke, X. Liu, Activation of Mps1 promotes transforming growth factor-beta-independent Smad signaling, J. Biol. Chem. 282 (2007) 18327–18338.

[36] S. Jusino, H.I. Saavedra, Role of E2Fs and mitotic regulators controlled by E2Fs in the epithelial to mesenchymal transition, Exp. Biol. Med. 244 (2019) 1419–1429.

[37] R. Miao, H. Luo, H. Zhou, G. Li, D. Bu, X. Yang, X. Zhao, H. Zhang, S. Liu, Y. Zhong, Z. Zou, Y. Zhao, K. Yu, L. He, X. Sang, S. Zhong, J. Huang, Y. Wu, R.A. Miksad, S. C. Robson, C. Jiang, Y. Zhao, H. Zhao, Identification of prognostic biomarkers in hepatitis B virus-related hepatocellular carcinoma and stratification by integrative multi-omics analysis, J. Hepatol. 61 (2014) 840–849.

[38] J.L. King, B. Zhang, Y. Li, K.P. Li, J.J. Ni, H.I. Saavedra, J.T. Dong, TTK promotes mesenchymal signaling via multiple mechanisms in triple negative breast cancer, Oncogenesis 7 (2018) 69.

[39] A. Molina, L. Velot, L. Ghouinem, M. Abdelkarim, B.P. Bouchet, A.C. Luissint, I. Bouhlel, M. Morel, E. Sapharikas, A. Di Tommaso, S. Honore, D. Braguer, N. Gruel, A. Vincent-Salomon, O. Delattre, B. Sigal-Zafrani, F. Andre, B. Terris, A. Akhmanova, M. Di Benedetto, C. Nahmias, S. Rodrigues-Ferreira, ATIP3, a novel prognostic marker of breast cancer patient survival, limits cancer cell migration and slows metastatic progression by regulating microtubule dynamics, Canc. Res. 73 (2013) 2905–2915.

[40] L. Zhao, D. Zhang, Q. Shen, M. Jin, Z. Lin, H. Ma, S. Huang, P. Zhou, G. Wu, T. Zhang, KIAA1199 promotes metastasis of colorectal cancer cells via microtubule destabilization regulated by a PP2A/stathmin pathway, Oncogene 38 (2019) 935–949.

[41] H.S. Lee, D.C. Lee, M.H. Park, S.J. Yang, J.J. Lee, D.M. Kim, Y. Jang, J.H. Lee, J. Y. Choi, Y.K. Kang, D.I. Kim, K.C. Park, S.Y. Kim, H.S. Yoo, E.J. Choi, Y.I. Yeom, STMN2 is a novel target of beta-catenin/TCF-mediated transcription in human hepatoma cells, Biochem. Biophys. Res. Commun. 345 (2006) 1059–1067.

[42] Q. Guo, N. Su, J. Zhang, X. Li, Z. Miao, G. Wang, M. Cheng, H. Xu, L. Cao, F. Li, PAK4 kinase-mediated SCG10 phosphorylation involved in gastric cancer metastasis, Oncogene 33 (2014) 3277–3287.

[43] S. Grieve, K. Ding, J. Moore, M. Finniss, A. Ray, M. Lees, F. Hossain, A. Murugesan, J. Agar, C. Acar, J. Taylor, F.A. Shepherd, T. Reiman, Immunohistochemical validation study of 15-gene biomarker panel predictive of benefit from adjuvant chemotherapy in resected non-small-cell lung cancer: analysis of JBR.10, ESMO Open 5 (2020).

[44] Y. Yang, S. Qi, C. Shi, X. Han, J. Yu, L. Zhang, S. Qin, Y. Gao, Identification of metastasis and prognosis-associated genes for serous ovarian cancer, Biosci. Rep. 40 (2020).

[45] M. Sherman, Recurrence of hepatocellular carcinoma, N. Engl. J. Med. 359 (2008) 2045–2047.

[46] R. Samarakoon, C.E. Higgins, S.P. Higgins, P.J. Higgins, Differential requirement for MEK/ERK and SMAD signaling in PAI-1 and CTGF expression in response to microtubule disruption, Cell. Signal. 21 (2009) 986–995.

[47] D.F. Quail, J.A. Joyce, Microenvironmental regulation of tumor progression and metastasis, Nat. Med. 19 (2013) 1423–1437.

[48] A.M. Cozzolino, T. Alonzi, L. Santangelo, C. Mancone, B. Conti, C. Steindler, M. Musone, C. Cicchini, M. Tripodi, A. Marchetti, TGFbeta overrides HNF4alpha tumor suppressing activity through GSK3beta inactivation: implication for hepatocellular carcinoma gene therapy, J. Hepatol. 58 (2013) 65–72.

[49] S. Faivre, L. Rimassa, R.S. Finn, Molecular therapies for HCC: looking outside the box, J. Hepatol. 72 (2020) 342–352.

[50] R.J. Akhurst, A. Hata, Targeting the TGFbeta signalling pathway in disease, Nat. Rev. Drug Discov. 11 (2012) 790–811.

[51] C. Dumontet, M.A. Jordan, Microtubule-binding agents: a dynamic field of cancer therapeutics, Nat. Rev. Drug Discov. 9 (2010) 790–803.

[52] Q. Zhou, A.K. Ching, W.K. Leung, C.Y. Szeto, S. Ho, P.K. Chan, Y. Yuan, P.B. Lai, W. Yeo, N. Wong, Novel therapeutic potential in targeting microtubules by nanoparticle albumin-bound paclitaxel in hepatocellular carcinoma, Int. J. Oncol. 38 (2011) 721–731.

[53] M. Deng, L. Li, J. Zhao, S. Yuan, W. Li, Antitumor activity of the microtubule inhibitor MBRI-001 against human hepatocellular carcinoma as monotherapy or in combination with sorafenib, Cancer Chemoth. Pharm. Times 81 (2018) 853–862.

[54] W. Yeo, H. Loong, Microtubule-targeting agents in oncology and therapeutic potential in hepatocellular carcinoma, OncoTargets Ther. 7 (2014) 575–585.

[55] P. Zhang, X. Ma, E. Song, W. Chen, H. Pang, D. Ni, Y. Gao, Y. Fan, Q. Ding, Y. Zhang, X. Zhang, Tubulin cofactor A functions as a novel positive regulator of ccRCC progression, invasion and metastasis, Int. J. Canc. 133 (2013) 2801–2811.

[56] S.Xie Tala, X. Sun, X. Sun, J. Ran, L. Zhang, D. Li, M. Liu, G. Bao, J. Zhou, Microtubule-associated protein Mdp3 promotes breast cancer growth and metastasis, Theranostics 4 (2014) 1052–1061.

[57] Y.Y. Jiang, L. Shang, Z.Z. Shi, T.T. Zhang, S. Ma, C.C. Lu, Y. Zhang, J.J. Hao, C. Shi, F. Shi, X. Xu, Y. Cai, X.M. Jia, Q.M. Zhan, M.R. Wang, Microtubule-associated protein 4 is an important regulator of cell invasion/migration and a potential therapeutic target in esophageal squamous cell carcinoma, Oncogene 35 (2016) 4846–4856.